EUROPHYSICS LETTERS 10 May 1994

Europhys. Lett., 26 (5), pp. 327-332 (1994)

Adaptive Recognition of a Chaotic Dynamics.

F. T. ARECCHI (*), G. BASTI (**) (***), S. BOCCALETTI (*) and A. L. PERRONE (***) (*_*)

(*) *Istituto Nazionale di Ottica - I-50125 Firenze*
Dipartimento di Fisica dell'Università - I-50125 Firenze
(**) *Università Gregoriana Pontificia - I-00187 Roma*
(***) *Istituto Nazionale di Fisica Nucleare, Sezione di Roma II - I-00133 Roma*
(*_*) *Dipartimento di Fisica, Università di Roma II - I-00133 Roma*

(received 9 February 1994; accepted in final form 22 March 1994)

PACS. 05.45 – Theory and models of chaotic systems.
PACS. 05.40 – Fluctuation phenomena, random processes, and Brownian motion.

Abstract. – The local variation rates of a chaotic dynamical system provide a means of stroboscopic observation at adjustable times which minimize the second variation of the coordinates. The sequence of strobing intervals carries global information on the dynamics, yielding a suitable indicator which discriminates deterministic from stochastic signals. Due to the adaptive nature of the strobing process, the characterization of this indicator requires a computational effort much smaller than statistical methods.

The standard observation of a (possibly continuous) dynamical system is performed by selecting a regular series of observation times (*i.e.* separated by a constant time interval) and plotting the evolution of the corresponding positions measured in some coordinate space. Based upon this geometrical series of data, one decides whether a signal is regular, or chaotic, or random.

Whenever the motion is confined within a finite region of space, an alternative approach consists in fixing a narrow observation window in the coordinate space. Registering only data within the window is a kind of stroboscopic inspection that provides a clustered set of geometric positions, but now the sequence of return times to the window is erratic if the dynamics is irregular. In more complex dynamics, with multibranched attractors, as *e.g.* in Lorenz case, the above argument fails in coincidence with jumps from one branch to the other; indeed, if the window selects positions of one branch, the stroboscopic series provides only partial information on the chaotic motion.

In this letter we show how to implement the stroboscopic inspection by adaptive windowing, which overcomes the above difficulty. This is done by exploiting the information provided by the local variation (expansion or contraction) rates. The stroboscopic time sequence that we extract provides not only useful indicators for the chaotic case, but it also permits discrimination between deterministic and stochastic dynamics.

Let us consider a dissipative dynamics $\dot{\boldsymbol{x}} = \boldsymbol{f}(\boldsymbol{x}, \mu)$, where $\boldsymbol{x}$ is a D-dimensional vector and μ a set of control parameters, and start by setting μ in order to have a stable periodic orbit of period $\bar{\tau}$. A $(D-1)$-dimensional Poincaré section intercepts the orbit at a point which repeats after a time $\bar{\tau}$. Suppose next that, by a change of μ, the orbit is destabilized toward a chaotic attractor.

A control tecnique introduced by Ott, Grebogi and Yorke (OGY) [1] consists in readjusting μ in such a way that the next iteration point lies on the stable manifold of the fixed point on the surface of section. A stroboscopic control method has also been proposed [2] whereby a small window is used for stabilizing one of the unstable periods of a chaotic attractor, but, since it relies on a window at a fixed position, it is unable to track signals jumping over widely separated phase space regions.

Rather than modifying the trajectory like in control methods [1,2], we aim at recognizing its unperturbed features. To this purpose, based upon the information provided by the local variation rates, we make the next observation interval shorter or longer than $\bar{\tau}$, in order to minimize *the variation in width* of the window which includes the two points at the extreme of the interval. This depends crucially on the fact that the expansion or contraction in a direction i cannot be monotonic in the course of time, since the attractor is confined within a finite support and hence the trajectory undergoes frequent twistings.

Precisely, for each coordinate axis i ($i = 1, \ldots, D$), we consider the variation

$$\delta x_i(t_{n+1}) = x_i(t_{n+1}) - x_i(t_n), \tag{1}$$

where $t_{n+1} - t_n = \tau_n$ is the n-th adjustable interval, to be specified. The goal of the adaptive windowing is to keep the separation between two successively observed coordinates as stable as possible, that is to minimize the variations of δx_i. In order to assign τ_{n+1}, we consider the local variation rate

$$\lambda_i(t_{n+1}) = \frac{1}{\tau_n} \log \left| \frac{\delta x_i(t_{n+1})}{\delta x_i(t_n)} \right|. \tag{2}$$

Here τ_n is the *minimum of all* $\tau_n^{(i)}$ corresponding to all different i, updated by the rule

$$\tau_{n+1}^{(i)} = \tau_n^{(i)}(1 - \mathrm{tgh}(g\lambda_i(t_{n+1}))). \tag{3}$$

The hyperbolic tangent function maps the whole range of $g\lambda_i$ into the interval $(-1, +1)$. The constant g, strictly positive, is chosen in such a way as to prevent $\tau_{n+1}^{(i)}$ from going to zero. It may be taken as an *a priori* sensitivity. A more sensible assignement would consist in looking at the unbiased dynamical evolution for a while and then taking a g value smaller than the reciprocal of the maximal λ recorded in that time span. Choosing a fixed g is like adjusting the connectivities of a neural network by a preliminary learning session, while adjusting g upon the information accumulated over a given number of previous time steps corresponds to considering g as a kind of long-term memory, as opposed to the short-term memory represented by the sequence of τ_n [3]. In summary, the steps of the algorithm are: observation of the data at t_{n+1}; evaluation of $\delta x_i(t_{n+1})$; evaluation of $\lambda_i(t_{n+1})$; updating of $\tau_{n+1}^{(i)}$; selection of $\min_i \tau_{n+1}^{(i)} = \tau_{n+1}$; determination of the new strobing time $t_{n+2} = t_{n+1} + \tau_{n+1}$.

This way, we obtain a sequence of observation times starting from given t_0 and $\bar{\tau}$:

$$t_0, t_1 = t_0 + \bar{\tau}, \qquad t_2 = t_1 + \tau_1, \ldots, t_{n+1} = t_n + \tau_n, \ldots, \tag{4}$$

according to which the variations of $\delta x_i(t_n)$ can be reduced below a preassigned value. The positions observed at the times t_n are confined within the adaptive window enfolding the trajectory; however, the time sequence (4) now includes the chaotic information which was in the original geometric sequence $\boldsymbol{x}(t)$.

The method here introduced has been applied to many chaotic situations as the Lorenz model (Lo) [4], the 3- and 4-dimensional Roessler model (called respectively Ro3 [5*a*] and Ro4 [5*b*] and the Mackey-Glass delay equation (MG) [6].

As an example, we report in fig. 1*a*) x_1 and δx_1 for Ro3. The window δx_i is confined within

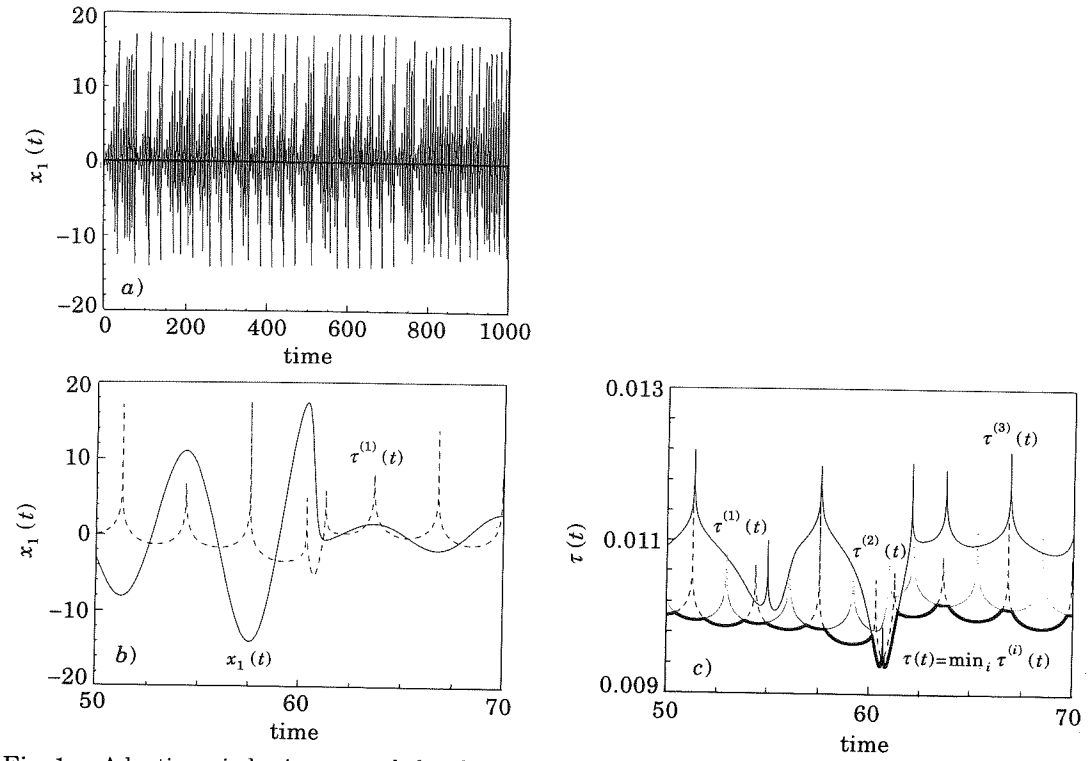

Fig. 1. – Adaptive windowing around the chaotic Ro3 attractor ($a = 0.2$, $b = 0.2$, $c = 9.0$). *a)* $x_1(t)$ and corresponding window $\delta x_1(t)$ (central thick line); $\tilde{\tau} = 0.01$, $g = 0.00015$. *b)* Expanded time section of $x_1(t)$ (solid line) and corresponding $\tau^{(1)}(t)$ (dashed line) evaluated by the adaptive algorithm (the vertical scale refers to $x_1(t)$, while $\tau^{(1)}(t)$ has been translated and expanded in order to emphasize its correlations with $x_1(t)$). *c)* Plots of $\tau^{(i)}(t)$ ($i = 1, 2, 3$), showing how the strobing interval $\tau(t) = \min_i \tau^{(i)}(t)$ is selected at any time step and then reinserted into the algorithm through eq. (2).

a range two orders of magnitude smaller than the variation range of $x_1(t)$. This reduction ratio depends on the chosen g and a compromise between maximal resolution (minimal window variation) and frequency of strobing operations has to be chosen. In fig. 1 the average strobing interval has a length of about 100 integration steps for the used Runge-Kutta method. In order to better illustrate how the algorithm works, we report (fig. 1*b*)) an expanded time section with $x_1(t)$ and the time $\tau^{(1)}$ corresponding to it. Figure 1*c*) shows how the strobing interval is selected at any step as the minimum of all $\tau^{(i)}$.

The sequence of strobing intervals contains the relevant information on the dynamics, thus we can characterize chaos as follows. Since in eq. (3) $|g\lambda_i| \ll 1$, then two successive τ_n must be strongly correlated. Thus, even though the τ_n may be spread over a rather wide support, the return map τ_{n+1} *vs.* τ_n clusters along the diagonal. Any appreciable deviation from the diagonal denotes the presence of uncorrelated noise. This is shown in fig. 2 where we plot the return map of the τ_n for Ro4 and for Ro4 with 1% noise.

The virtue of the adaptive technique consists in an optimized choice among a large number of possibilities offered by the irregular dynamics. If applied to a regular orbit, the method becomes critical, due to the singular invariant distribution of the periodic attractor. In such a case the fixed point τ^* of the τ_{n+1} *vs.* τ_n map displays a structural instability inducing a slow drift. To correct for this, we must recur to the second adaption level sketched above, that is, change g upon the information associated with the previous time steps. This is demonstrated

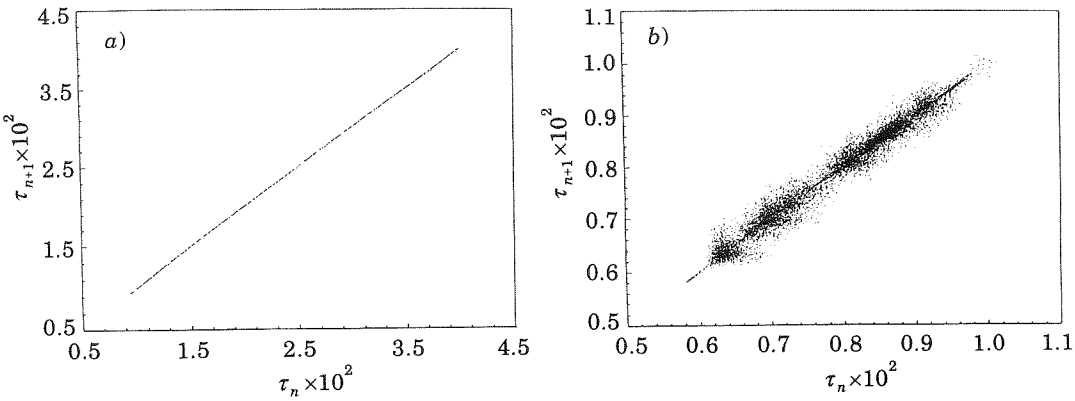

Fig. 2. – Return maps τ_{n+1} *vs.* τ_n for *a*) Ro4 and *b*) Ro4 with an additional 1% white noise. Initial conditions: $x(0) = -20$, $y(0) = z(0) = 0$, $w(0) = 15$, $g = 0.000048$.

with reference to a forced Duffing oscillator

$$\ddot{x} + 0.154\dot{x} - x + 4x^3 = 0.2\cos(1.1t). \tag{5}$$

The selected parameters correspond to a stable periodic orbit. For fixed g, τ^* runs away. This anomaly disappears by updating g every 30 observer time steps, with the rule that the new g is given by

$$g = g_0 + \frac{1}{\sum |\lambda_i|}. \tag{6}$$

Here the sum is over all i and over all the previous 30 time intervals, so that it includes the maximum $|\lambda_i|$ occuring in that time span, and g_0 is a safety term that provides a minimum sensitivity in case $1/(\sum |\lambda_i|)$ gets close to zero.Figure 3 displays the τ sequences for about 400 forcing periods, showing the reliability of our method.

To extract a quantitative indicator from the return map τ_{n+1} *vs.* τ_n, we evaluate the average deviation of the observation times away from the diagonal. This should provide an estimate for the maximum Liapunov exponent $\Lambda_{\max}$, since, by eq. (3), the normalized deviation yields the local rate. By direct use of eq. (2), we propose the following indicator:

$$\eta = \frac{1}{M}\sum_{+}\sum_{i}\lambda_i(t_n), \tag{7}$$

where $\sum_{+}$ accounts only for the n_+ cases for which $\min \tau_{n+1}^{(i)} \leqslant \min \tau_n^{(i)}$, $\sum_i$ runs over all m dimensions of the phase space, and $M = Nm$, where $N = n_+ + n_-$ is the total number of strobing observations ($n_{+(-)}$ is the number of the shrinking (stretching) strobing intervals). The soundness of eq. (7) is shown by comparing η with $\Lambda_{\max}$ in the case of Ro3. The positive Liapunov exponent of Ro3 with $a = b = 0.2$, $c = 5.7$ and for $N_d = 40\,000$ data turns out to be [7] $\Lambda_{\max} = 0.072 \pm 0.001$ by the Benettin *at al.* algorithm [8] and $\Lambda_{\max} = 0.075 \pm 0.005$ by the Sano-Sawada algorithm [9]. By applying our method with a sensitivity $g = 0.00038$ to the same system ($\bar{\tau} = 6.3$) and evaluating η for an increasing number of data, η reaches a plateau beyond 6000 data. Its average between 8000 and 12 000 data, with three times the standard deviation, is $\eta = 0.0722 \pm 0.0003$. We obtain similar reductions in the data number and in the standard deviation with respect to ref. [7] also in the case of Ro4 and Lo, as will be reported elsewhere.

So far we have dealt with an assigned model as Ro3, Ro4 and Lo. A more difficult task is to characterize an empirical time series, in order to discriminate whether it corresponds to a

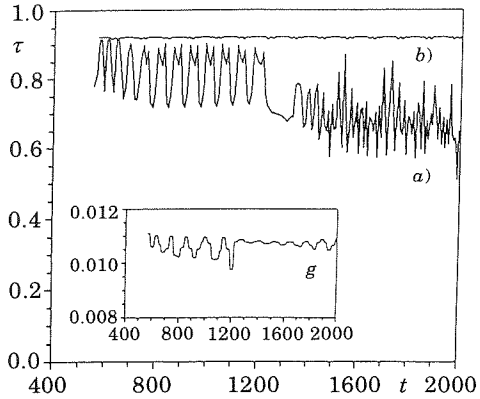

Fig. 3.

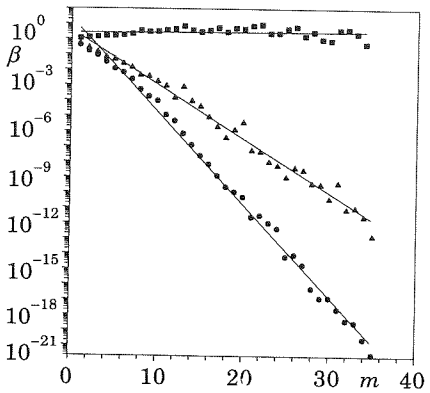

Fig. 4.

Fig. 3. – Strobing time *vs.* absolute time for a forced oscillator on a periodic orbit (eq. (5)). *a*) Runaway solution; fixed sensitivity $g = 0.05$. *b*) Stable solution $\tau = \tau^* \simeq 0.92$; sensitivity adjusted every 30 time steps via eq. (6), as shown in the inset ($g_0 = 0.005$).

Fig. 4. – β plots *vs.* embedding dimension m. Squares: white noise, triangles: surrogate of MG, circles: MG attractor. For all cases $g = 0.0048$. Solid lines are exponential fits $\exp[Am]$, with $A = 0.039$ for white noise, $A = -0.526$ for the surrogate of MG and $A = -0.987$ for MG.

deterministic or stochastic phenomenon. To this purpose, we embed our data series in spaces of increasing dimensions.

A very stringent test is represented by MG:

$$\dot{x} = -0.1x(t) + \frac{0.2x(t-\tau)}{1 + x(t-\tau)^{10}} . \tag{8}$$

With $\tau = 100$ it corresponds to ~ 7.5-dimensional chaotic dynamics [10].

Let us consider the time series for MG, for a pure white noise with r.m.s. fluctuations as MG, and for a random phase time series having the same spectral power as MG (surrogate) [11].

For an empirical series of data with no *a priori* information, a discrimination between determinism and noise is provided by the following indicator:

$$\beta = \frac{1}{N} \sum_n \left| \prod_{i=1}^{m} \lambda_i(t_n) \right| . \tag{9}$$

Its heuristic meaning emerges from the following considerations. Expanding eq. (2) to first order and referring to the unit time step $\tau_n = 1$, we can write $\lambda_i(t_{n+1}) = (\delta x_i(t_{n+1}) - \delta x_i(t_n))/\delta x_i(t_n)$. We now evaluate the variation over the unit time of the volume $V_n = \prod_{i=1}^{m} \delta x_i(t_n)$ made by all m measured variations at time t_n. The relative variation rate $r_n = (V_{n+1} - V_n)/V_n$ is given by

$$r_n = \sum_i \lambda_i + \sum_{i \neq j} \lambda_i \lambda_j + \ldots + \prod_i \lambda_i . \tag{10}$$

Summing up over all directions of phase space, we introduce the directional averages

$$\langle \lambda \rangle = \frac{1}{m} \sum_i \lambda_i , \qquad \langle \lambda^2 \rangle = \frac{2}{m(m-1)} \sum_{i \neq j} \lambda_i \lambda_j , \qquad \text{etc.}$$

As we further sum over all n up to N, the twisting along the chaotic trajectory makes all directions statistically equivalent, thus in $\sum_n r_n$ we can replace $\langle \lambda^k \rangle$ by $\langle \lambda \rangle^k$ for $2 \leqslant k \leqslant m$. In the case of stochastic noise, since variations over successive time steps are uncorrelated, $\delta x(t_{n+1}) - \delta x(t_n) \simeq \delta x(t_n)$ and $\langle \lambda \rangle$ is close to 1, so that $\langle \lambda \rangle^m = O(1)$. Instead, for a deterministic dynamics two successive steps are strongly correlated, hence $\langle \lambda \rangle < 1$, and the last term of eq. (10), that is $\langle \lambda^m \rangle \sim \langle \lambda \rangle^m = \exp[-m \log(1/\langle \lambda \rangle)]$ yields the most sensitive test.

Based on these considerations, we take the sum over the N trajectory points of the last term of eq. (10) as the β indicator displayed in eq. (9). In view of what said above, β scales like $\exp[-m]$ for a deterministic signal (apart from a factor $O(1)$ in the exponent) whereas it scales as $\exp[0]$ for noise and as $\exp[0.5\,m]$ for surrogate, since one-half of the total number of degrees of freedom (phases of the Fourier components) scales like noise and the other half (amplitudes) scales like the deterministic signal.

Figure 4 shows the β plots *vs.* m for MG and its surrogate as well as for white noise. In order to estimate the minimal number $S(m)$ of data necessary for any value m, we start from a very large value S and reduce it until we obtain a deviation $\Delta\beta/\beta \simeq 10\%$. With this definition the number $S(m)$ of data necessary for MG scales as $S(m) = a + bm$, with $a \simeq 10\,000$ and $b \simeq 3000$.

Comparing our adaptive recognition with statistical methods based upon the assignement of a probability measure in phase-space, as counting the number of neighbours within a given distance from each phase-point [12] or the distribution of distances for closest neighbours [13], we easily realize that, for S data points, the number of computing operations scales as S in our case and as S^2 in the statistical cases. Furthermore, to assure a good resolution in m embedding dimensions, statistical methods require that $S(m)$ increase exponentially in m, whereas our adaptive strategy is based on variation rates along the coordinate axes and hence our $S(m)$ scales linearly with m as shown above. Similar comparative remarks hold also for recent tests for determinism [14], based on exploring the evolution of a neighborhood of close points.

* * *

We thank R. KAPRAL, R. LIVI and A. POLITI for helpful discussions. Work partly supported by EEC Contract No.: SC1-CT91-0697.

REFERENCES

[1] OTT E., GREBOGI C. and YORKE J. A., *Phys. Rev. Lett.*, **64** (1990) 1196; AUERBACH D., GREBOGI C., OTT E. and YORKE J. A., *Phys. Rev. Lett.*, **69** (1992) 3479.
[2] PENG B., PETROV V. and SHOWALTER K., *J. Phys. Chem.*, **95** (1991) 4957; HUNT E. R., *Phys. Rev. Lett.*, **67** (1991) 1953.
[3] GROSSBERG S., *Neural Networks*, **1** (1988) 17.
[4] LORENZ E. N., *J. Atmos. Sci.*, **20** (1963) 130.
[5] *a*) ROESSLER O. E., *Phys. Lett. A*, **57** (1976) 397; *b*) ROESSLER O. E., *Phys. Lett. A*, **71** (1979) 155.
[6] MACKEY M. C. and GLASS L., *Science*, **197** (1977) 287.
[7] KRUEL TH.-M., EISWIRTH M. and SCHNEIDER F. W., *Physica D*, **63** (1993) 117.
[8] BENETTIN G., GALGANI L., GIORGILLI A. and STRELCYN J.-M., *Meccanica*, **15** (1980) 9.
[9] SANO M. and SAWADA Y., *Phys. Rev. Lett.*, **55** (1985) 1082.
[10] FARMER J. D., *Physica D*, **4** (1982) 366; GRASSBERGER P. and PROCACCIA I., *Physica D*, **9** (1983) 189.
[11] THEILER J. *et al.*, in *Nonlinear Modeling and Forecasting*, edited by M. CASDAGLI and S. EUBANK (Addison-Wesley, Reading, Mass.) 1992.
[12] GRASSBERGER P. and PROCACCIA I., *Phys. Rev. Lett.*, **50** (1983) 346.
[13] BADII R. and POLITI A., *Phys. Rev. Lett.*, **52** (1984) 1661.
[14] KAPLAN D. T. and GLASS L., *Phys. Rev. Lett.*, **68** (1992), 427; WAYLAND R., BROMLEY D., PICKETT D. and PASSMANTE A., *Phys. Rev. Lett.*, **70** (1993) 580.